第 36 卷 第 11 期　　无 机 材 料 学 报　　Vol. 36 No. 11
2021 年 11 月　　Journal of Inorganic Materials　　Nov., 2021

Article ID: 1000-324X(2021)11-1231-06　　**DOI:** 10.15541/jim20210150

Microstructure and Properties of ZrO_2-AlN Composite Ceramics by Microwave Sintering

MU Tinghai[1,2], XU Wentao[2,3], LING Junrong[2], DONG Tianwen[2], QIN Zixuan[2], ZHOU Youfu[2,3]

(1. College of Chemistry and Materials Science, Fujian Normal University, Fuzhou 350007, China; 2. Key Laboratory of Optoelectronic Materials Chemistry and Physics, Fujian Institute of Research on the Structure of Matter, Chinese Academy of Sciences, Fuzhou 350002, China; 3. Fujian Science & Technology Innovation Laboratory for Optoelectronic Information of China, Fuzhou 350108, China)

Abstract: Zirconia (ZrO_2) ceramics have excellent mechanical properties, but its application is limited by ZrO_2-AlN low thermal conductivity (TC). Zirconia-aluminum nitride (AlN) composite ceramics ZrO_2-AlN with high TC were designed and successfully fabricated by microwave sintering. After optimization of preparation conditions, the reaction between two substances was inhibited and the dense composite (relative density>99%) was obtained. The microstructure evolution, thermal behavior and mechanical properties were investigated in detail. The room temperature thermal conductivity, thermal diffusion coefficient and thermal capacity of ZrO_2-AlN composites increase with AlN content increasing, reaching 41.3 W/(m·K), 15.2 mm^2/s and 0.6 J/(g·K), respectively. Such ZrO_2-AlN composites with high thermal conductivity and improved thermal shock resistance have broad application prospects in the field of high temperature heat exchange materials of energy systems.

Key words: zirconia; aluminum nitride; composite ceramic; microwave sintering; thermal conductivity

ZrO_2 has intriguing advantages including excellent mechanical properties, high temperature endurance, outstanding chemical stability and good ionic conductivity. ZrO_2-based ceramics are industrially important and widely applied as the structural and functional materials, including cutting tools, bearing parts, thermal barrier and solid oxide fuel cells. It is well known that ZrO_2 is polymorphs and exists in monoclinic (m), tetragonal (t) or cubic (c) crystal phases at different temperatures or sizes[1-3]. The c-ZrO_2 has been of interest as an inert matrix nuclear fuel material for nuclear energy systems[4], due to its low neutron absorption cross-section[5], structural similar to nuclear fuel UO_2[6], high resistance to amorphization and thermal stability. The room temperature stabilized cubic form can be obtained by the substitution of Y^{3+} for Zr^{4+} ions[7]. Its response under heavy ion radiation has been studied, for the nuclear and electronic stopping energy range. However, low thermal conductivity (1.8 W/(m·K)), high thermal expansion coefficient (resulting in poor thermal shock resistance) and brittleness of ZrO_2 ceramics[8] are still barriers for their use as confinement matrix material.

In order to stabilize the cubic structure of ZrO_2 at room temperature, pure ZrO_2 materials are doped by oxides. The cations with a radius larger than Zr^{4+} are introduced to replace Zr^{4+} lattice points, forming a substitute solid solution, thereby maintaining the obtained doped solid solution at room temperature. Commonly used stabilizing cations include Y^{3+}[7], Ce^{3+}, Mg^{2+}, Ca^{2+}, *etc*.

Composite materials are expected to overcome the inherent shortcomings of single-phase ceramics and bring about an overall improvement in structure and functional characteristics[9-11]. For example, Al_2O_3-ZrO_2 system[12] is one of the most studied and promising ceramic composites. Al_2O_3 with a relatively higher thermal conductivity (30 W/(m·K)) as compared with UO_2[6] can be chosen as the heat-conducting phase. Nevertheless, the thermal conductivity of composite materials is still not ideal. On the other hand, due to mutual reactions, there are few studies on the zirconia composite with non-oxide components.

Aluminum nitride (AlN) has high thermal conductivity (320 W/(m·K))[13], high temperature resistance (2450 ℃), high resistance to metal melt corrosion, low density

---

Received date: 2021-03-11; **Revised date:** 2021-04-12; **Published online:** 2021-05-10
Foundation item: Strategic Priority Research Program of the Chinese Academy of Sciences (XDB20010300, XDA21010204); Adv. Energy Sci. & Technol. Guangdong Lab (Open laboratory)
Biography: MU Tinghai (1995–), male, Master candidate. E-mail: mutinghai@fjirsm.ac.cn
牟庭海(1995–)，男，硕士研究生. E-mail: mutinghai@fjirsm.ac.cn
Corresponding author: ZHOU Youfu, professor. E-mail: yfzhou@fjirsm.ac.cn
周有福，研究员. E-mail: yfzhou@fjirsm.ac.cn

(3.26 g/cm^3) and low thermal expansion coefficient (4.6×10^{-6}/℃)[14]. It is an excellent component, which can significantly improve the thermal conductivity and thermal shock resistance of composite materials.

Motivated by the above mentioned, herein AlN was introduced and the corresponding ZrO_2-AlN composite ceramics were prepared successfully at 1350 ℃ by microwave sintering. Compared with conventional sintering, the microwave sintering can cause internal molecular vibrations under electromagnetic radiation, further leading to self-heating from the core, resulting in lower sintering temperature and finer microstructure of specimen. The phase composition and morphology evolution were identified by X-ray diffraction (XRD) and scanning electron microscope (SEM), respectively. Furthermore, the effect of the AlN on the thermal and mechanical properties was investigated and discussed. Optimal ZrO_2-AlN composite owns thermal conductivity up to 41.3 W/(m·K).

1 Experimental

Raw materials ZrO_2 and AlN were commercially available and used as received. Commercially available Y_2O_3 (8mol% of ZrO_2), Al, CaF_2, TiO_2 and B (5wt% of AlN and the proportion of each part is 3 : 3 : 1 : 0.08) were used as sintering additives[13]. The mixture of ZrO_2, AlN and sintering additives were milled in a planetary ball milling machine (XGB4, Nanjing Boexpress Co., China) with ethanol as the medium. The resulted slurry was dried in vacuum and sieved. Pellets were prepared by uniaxial pressing followed by cold isostatic pressing (CIP). The compositions of the ceramic samples are shown in Table 1. The pellets were sintered in the microwave sintering furnace (Hunan Zhongsheng Co., China) at 1350 ℃ for 4 h under N_2 atmosphere. The temperature program of sintering process is shown in Fig. 1. After microwave sintering, the samples were cooled naturally to room temperature and collected. The obtained ceramics were grinded for the further characterization.

The density of ceramics was measured by the Archimedes method. Vickers hardness was measured on polished surface with a load of 9.8 N for 15 s using a microhardness tester (HX-1000TM). Fracture toughness measurement was performed using indentation method, and results were obtained by the formula (1)[15]:

$$K_{(\text{IC-Niihara})} = 0.0181E^{0.4}{H_v}^{0.6}a(c-a)^{-0.5} \qquad (1)$$

where E and H_v are elastic modulus and Vickers hardness of the sample, while c and a are the half-length of crack cracking and the half-length of diagonal indentation of the sample. Standard test pieces (3 mm×4 mm×36 mm) were obtained by using cutting machine and polishing. Three-point-bending method was used to measure the flexure strength on an electronic universal testing machine (UTM17093) with a span of 20 mm at a crosshead speed of 0.5 mm/min. X-ray diffractometer (CuKα, 30 kV/10 mA, Rigaku Miniflex-600, Tokyo, Japan) and SEM (Helios, G4 CX, Germany) were employed to study the surface and fracture morphology, respectively. The samples for the analyses of thermal diffusivity were in the dimension of 10 mm×10 mm×2 mm. The thermal conductivity was measured using a laser thermal conductivity meter (Netzsch, LFA457, Germany) and calculated[16].

2 Results and discussion

2.1 Phase analyses

As shown in Fig. 2, the powders are mixed, containing some AlN and a large amount of ZrO_2 with monoclinic and tetragonal phases as received. As shown in Fig. 3, the EDS mapping reflects that the powder has been mixed evenly after ball milling. The XRD patterns of samples sintered at 1350 ℃ are shown in Fig. 4(a). For ZAN-0, c-ZrO_2 is the predominant phase with a bit t-ZrO_2. ZrO_2-AlN composite ceramics are composed of ZrO_2 and AlN, and the intensity of the diffraction peak of AlN phase increases with its content increasing. The monoclinic zirconia existing in the raw material powder is converted into a tetragonal or cubic phase at high temperature and keeps stable at room temperature after cooling. The XRD patterns of ZAN-2 with W_{ZrO_2}/W_{AlN}=9 : 1 sintered from 1300 to 1400 ℃ are shown in Fig. 4(b). c-ZrO_2 and AlN are the only two phases at 1300 and 1350 ℃. With the

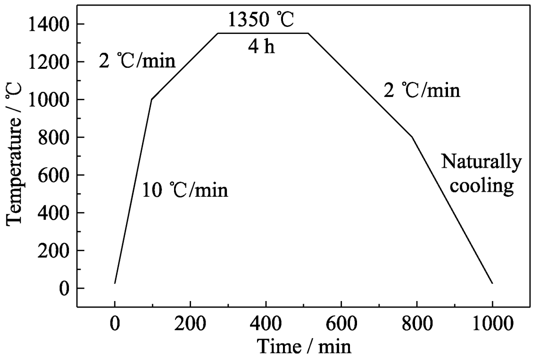

Fig. 1 Sintering process of ZrO_2-AlN composite ceramic

Table 1 Compositions of samples

Specimen	Composition
ZAN-0	100%ZrO_2
ZAN-1	95wt%ZrO_2+5wt%AlN
ZAN-2	90wt%ZrO_2+10wt%AlN
ZAN-3	85wt%ZrO_2+15wt%AlN
ZAN-4	80wt%ZrO_2+20wt%AlN

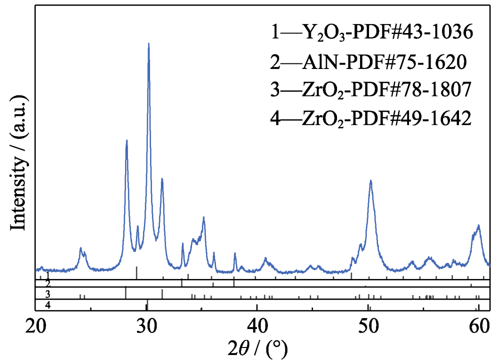

Fig. 2　XRD pattern of raw material powder after ball milling and mixing

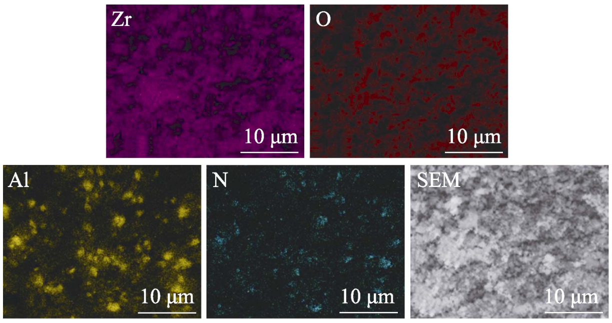

Fig. 3　EDS mapping images of mixed powder after ball milling

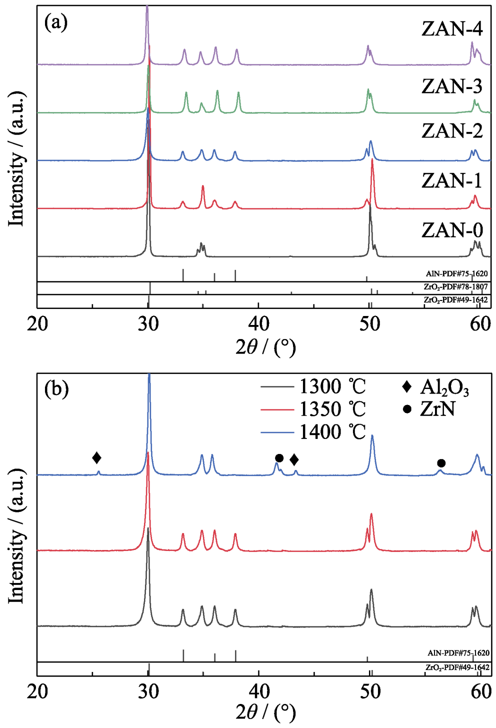

Fig. 4　XRD patterns of ZrO_2-AlN composite ceramics sintered at 1350 ℃ (a) and at different temperatures (b)

temperature increasing to 1400 ℃, two byproducts including ZrN and Al_2O_3 appear, which are attributed to the reaction of ZrO_2 and AlN[17]:

$$1.5ZrO_2 + 2AlN \rightarrow 1.5ZrN + Al_2O_3 + 0.25N_2 \qquad (2)$$

ZrO_2 and AlN are the major phases in the specimens sintered at 1350 ℃ (Fig. 4(a)), while trace amount of ZrN and Al_2O_3 emerged at higher sintering temperature (Fig. 4(b)).

2.2　Mechanical properties

The relative densities of the composites with different AlN contents are shown in Fig. 5(a). The relative density of all samples is higher than 99%, and the pure zirconia has the highest relative density of 99.7%. With the increase of AlN content, the relative density of composites decreases gradually. As shown in Table 2, the relative density of the ZAN-2 samples prepared under different ball milling processes and cold isostatic pressing (CIP) pressures showed different changes, and the ZAN-2 samples prepared by the 1# process had the highest relative density. The sintering temperature is 1350 ℃, which is higher than the melting point of Al. During the sintering process, Al is molten and further transient liquid phase sintered, promotes the densification of the composites. With the increase of AlN, AlN grains are not uniformly distributed in the matrix, which weakens the inhibition effect on ZrO_2 grains in the matrix, leading to the abnormal growth of some ZrO_2 grains. In addition, AlN also affects the contact between ZrO_2 grains and affects the shrinkage which plays an inhibiting role in the sintering. Thus, the relative density of composite ceramic decreases with the increase of AlN.

Fig. 5(b) demonstrates the change of Vickers hardness of ZrO_2-AlN composite ceramics with different AlN contents. With the increase of AlN, the Vickers hardness of composite ceramics decrease from 14.3 GPa (0) to 9.8 GPa (20wt%) due to the hardness of AlN being lower than that of matrix ZrO_2. According to the composite law of mechanical properties, the higher content of AlN, the lower hardness of composite is. At the same time, hardness is a very sensitive property to compactness. With the further increase of AlN, the compactness decreases and the hardness decreases correspondingly.

Fig. 5(c,d) display the changes of fracture toughness and flexural strength of ZrO_2-AlN composite ceramics with AlN contents. With the increase of AlN addition, both fracture toughness and bending strength of ZrO_2-AlN composite ceramics show a decreasing trend. This can be assigned to the fact that the sintering temperature of AlN is higher than that of ZrO_2. Some AlN particles stacked with each other grow abnormally, while ZrO_2 particles in the matrix grow to a certain extent at high temperature due to the lack of effective inhibition originating from AlN grains around. Therefore, with AlN content in the matrix increasing, fracture toughness and bending strength of composites decrease.

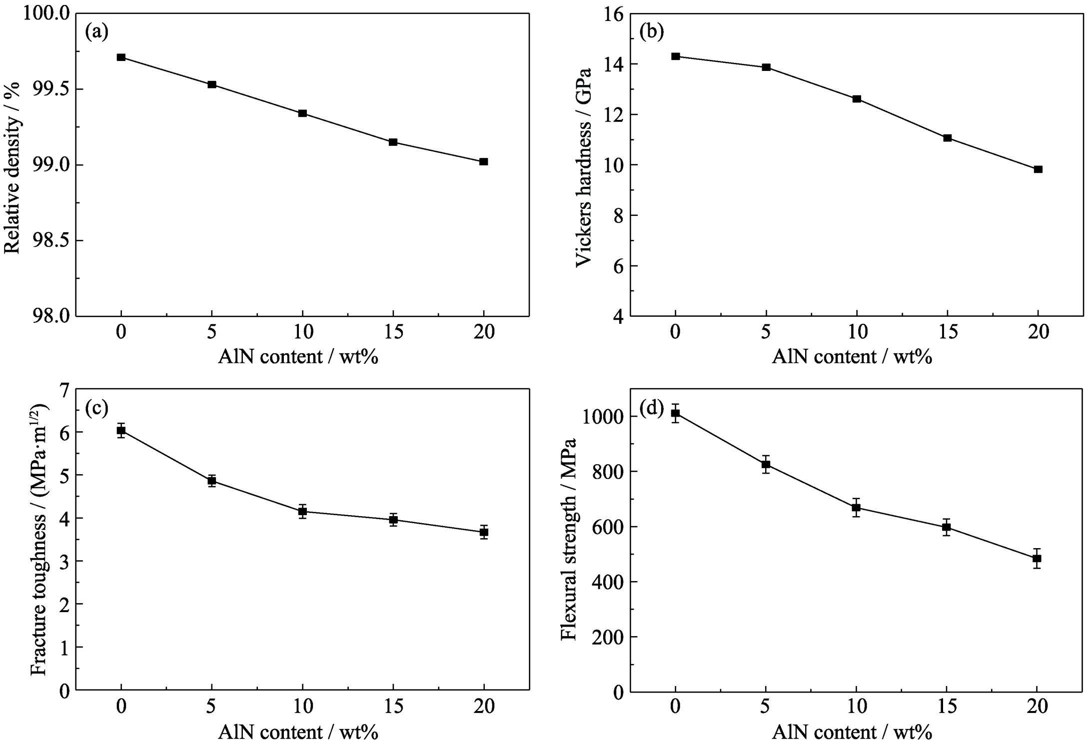

Fig. 5 Relative density and mechanical behavior of different ZrO_2-AlN composite ceramics
(a) Relative density; (b) Vickers hardness; (c) Fracture toughness; (d) Flexural strength

Table 2 Relative density of ZAN-2 sample prepared by different CIP pressure and ball milling processes

Sample	Rotating speed/($r\cdot min^{-1}$)	Rotating time/h	Pressure/MPa	Relative density/%
1#	250	24	200	99.3
2#	250	12	200	98.5
3#	200	24	200	98.9
4#	250	24	100	98.1

2.3 Microstructural characterization

In order to investigate the microstructure evolution of ZrO_2-AlN composite ceramics, SEM images of the ZAN-2 sample after acid corrosion were shown in Fig. 6(a,b). The sample only displays ZrO_2 and AlN phases without any impurity phases, which is consistent with the XRD results. The brighter areas are ZrO_2 phases and the darker areas are AlN phases. Furthermore, the ZrO_2 phase is well developed, and AlN phase is distributed at the boundaries of ZrO_2, which is helpful to maintain lattice integrity of ZrO_2 and reduce lattice defects. The AlN is distributed orderly in ZrO_2 substrate, which can improve the microstructure uniformity of composite ceramics. It is noteworthy that a small number of pores exist in the SEM image, which confirms the fact of low relative density. Fig. 6(c,d) are the cross-section SEM images. It can be found that the particles are tightly packed with intact grains and clean grain boundaries. At the same time, the fracture mode of ZrO_2-AlN composite ceramics is mainly transcrystalline fracture, and the fracture toughness is lower than that of pure ZrO_2 ceramics. The crack propagated at the grain boundary with microscopical deflection and grain pullout. The crack deflection may be favorable for the toughening of composites. As a result, the incorporation of AlN makes the microstructure of ZrO_2 matrix composites passivating and heterogeneity. Thus,

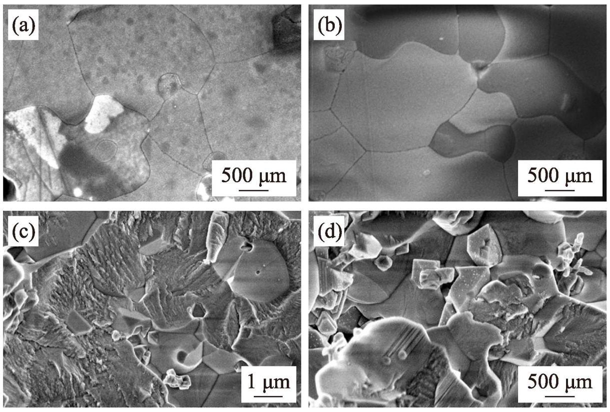

Fig. 6 SEM images of the polished surfaces (a, b) and fracture surfaces (c, d) of ZAN-2 sample

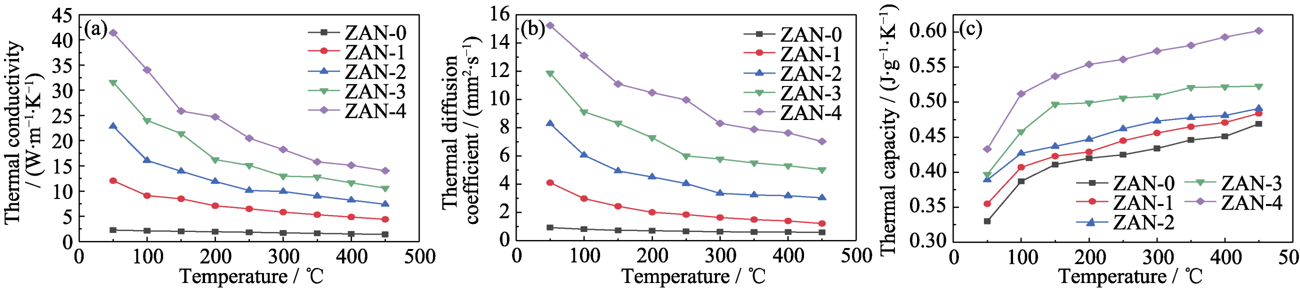

Fig. 7　Thermal performance of ZrO_2-AlN composite ceramics with different AlN contents

(a) Thermal conductivity; (b) Thermal diffusion coefficient; (c) Thermal capacity

the mechanical properties of the composites are reduced in comparison with that of pure ZrO_2.

2.4　Thermal analysis

The concept of phonon can be adopted to explain the heat conduction phenomenon of materials[18]. The thermal conductivity of ceramic material is proportional to the average phonon free path[19]. As shown in Fig. 7(a), the thermal conductivity of composite ceramics at 50 ℃ gradually increases from 2.2 W/(m·K) (ZAN-0) to 41.3 W/(m·K) (ZAN-4), which is attributed to the thermal conductivity at room temperature of ZrO_2 (2.2 W/(m·K)) is lower than that of AlN (320 W/m·K). In addition, with the temperature increasing, the thermal conductivity of composite ceramic decreases gradually. The kinetic energy of the phonons and the vibration increases with the increase of temperature, which leads to the increase of collision probability between phonons and further the decrease of thermal conductivity[20]. The thermal diffusion coefficients of different ZrO_2-AlN composite ceramics are shown in Fig. 7(b). The thermal diffusion coefficient of the composite ceramic at 50 ℃ gradually increases from 0.9 mm^2/s (ZAN-0) to 15.2 mm^2/s (ZAN-4). In addition, the thermal diffusion coefficient of composite ceramic decreases gradually as the temperature increases. The main reason is that the increase of temperature will improve the difficulty of temperature homogenization of ceramic material, so the thermal diffusivity will further gradually decrease[21]. Fig. 7(c) shows the change of thermal capacity of ZrO_2-AlN composite ceramic at various temperatures. At the low temperature range, the thermal capacity of composite ceramics increases sharply with the increase of temperature. When the temperature is higher than 250 ℃, the thermal capacity increases slowly with temperature increasing. Debye model under the condition of simple harmonic approximation indicates that the thermal capacity of ceramics is $\propto T^3$ at low temperature, while the thermal capacity gradually tends to a constant value at high temperature[22-23]. The above result is consisted well with this model.

3　Conclusions

AlN was introduced into zirconia matrix as the toughening phases by novel microwave sintering. The mechanical and thermal property of the obtained ZrO_2-AlN composite ceramics were analyzed. With the increase of AlN content, the relative density of ZrO_2-AlN composite ceramic gradually decreases. ZrO_2-AlN composite ceramics with 20wt% AlN obtains the highest thermal conductivity (41.3 W/(m·K)), the maximum thermal diffusion coefficient (15.2 mm^2/s) at room temperature and the best thermal capacity (0.6 J/(g·K)).

References:

[1] LI J, PENG J, GUO S, *et al.* Thermodynamic calculations of t to m martenstic transformation of ZrO_2-CaO binary system. *Ceramics International*, 2012, **38(4):** 2743–2747.

[2] LI K, WANG D, CHEN H, *et al.* Normalized evaluation of thermal shock resistance for ceramic materials. *Journal of Advanced Ceramics*, 2014, **3(3):** 250–258.

[3] YOSHINAGA M, SASAKI T, KOBAYASHI N. Effect of microwave irradiation for crystallization behavior of yttria-stabilized zirconia system. *Journal of the Ceramic Society of Japan*, 2019, **127(10):** 767–772.

[4] MALYI O I, WU P, KULISH V V, *et al.* Formation and migration of oxygen and zirconium vacancies in cubic zirconia and zirconium oxysulfide. *Solid State Ionics*, 2012, **212:** 117–122.

[5] WANG L, LIANG T. Ceramics for high level radioactive waste solidification. *Journal of Advanced Ceramics*, 2012, **1(3):** 194–203.

[6] LI B, YANG, CHU M, *et al.* Ti_3SiC_2/UO_2 composite pellets with superior high-temperature thermal conductivity. *Ceramics International*, 2018, **44(16):** 19846–19850.

[7] HOLGATE C S, SEWARD G G E, ERICKS A R, *et al.* Dissolution and diffusion kinetics of yttria-stabilized zirconia into molten silicates. *Journal of the European Ceramic Society*, 2021, **41(3):** 1984–1994.

[8] MEBRAHITOM ASMELASH G, MAMAT O, AHMAD F, *et al.* Thermal shock and fatigue behavior of pressureless sintered Al_2O_3-SiO_2-ZrO_2 composites. *Journal of Advanced Ceramics*, 2015, **4(3):** 190–198.

[9] DONG K F, MO W Q, JIN F, *et al.* Effect of TiN-ZrO_2 intermediate layer on the microstructure and magnetic properties of FePt and FePt-SiO_2-C thin films. *Journal of Magnetism and Magnetic Materials*, 2017, **432:** 323–329.

[10] JI Y, FU R, LV J, *et al.* Enhanced bonding strength of Al_2O_3/AlN

ceramics joined *via* glass frit with gradient thermal expansion coefficient. *Ceramics International*, 2020, **46(8):** 12806–12811.

[11] LAZAR A, KOSMAC T, ZAVASNIK J, *et al.* TiN-nanoparticulate-reinforced ZrO_2 for electrical discharge machining. *Materials (Basel)*, 2019, **12(17):** 2788–2802.

[12] ESMAEILZAEI A, SAJJADI S A, MOLLAZADEH BEIDOKHTI S, *et al.* Rapid consolidation of Al_2O_3-TiO_2-Co nanocermets *via* spark plasma sintering of Co-coated ceramic particles. *Journal of Alloys and Compounds*, 2019, **771:** 79–88.

[13] OKAZAKI H, KOBAYASHI R, HASHIMOTO R, *et al.* Thermal conductivity and mechanical strength of low-temperature-sintered aluminum nitride ceramics containing aluminum nitride whiskers. *Journal of the Ceramic Society of Japan*, 2020, **128(11):** 991–994.

[14] YEH CT, TUAN W H. Oxidation mechanism of aluminum nitride revisited. *Journal of Advanced Ceramics*, 2017, **6(1):** 27–32.

[15] MIYAZAKI H, YOSHIZAWA YI. Correlation of the indentation fracture resistance measured using high-resolution optics and the fracture toughness obtained by the single edge-notched beam (SEPB) method for typical structural ceramics with various microstructures. *Ceramics International*, 2016, **42(6):** 7873–7876.

[16] TANAKA I. Impacts of first principles calculations in engineering ceramics. *Journal of the Ceramic Society of Japan*, 2016, **124(8):** 791–795.

[17] LU Y, YUAN Z, SHEN H, *et al.* High-temperature phase relations of ZrN-ZrO_2-Y_2O_3 ternary system. *Journal of Advanced Ceramics*, 2018, **7(4):** 388–391.

[18] CALLAWAY J. Model for lattice thermal conductivity at low temperatures. *Physical Review*, 1959, **113(4):** 1046–1051.

[19] TAO Y, LIU C, CHEN W, *et al.* Mean free path dependent phonon contributions to interfacial thermal conductance. *Physics Letters A*, 2017, **381(22):** 1899–1904.

[20] SLACK G A. Nonmetallic crystals with high thermal conductivity. *J. Phys. Chem. Solids*, 1972, **34:** 321–335.

[21] HONG H, KIM J, KIM T I. Effective assembly of nano-ceramic materials for high and anisotropic thermal conductivity in a polymer composite. *Polymers*, 2017, **9(9):** 413.

[22] CHEN H, WEI J, CHEN Y, *et al.* Theoretical investigation of the mechanical and thermodynamic properties of titanium pernitride under high temperature and high pressure. *Journal of Alloys and Compounds*, 2017, **726:** 1179–1185.

[23] NOVIKOV V V. Debye-Einstein model and anomalies of heat capacity temperature dependences of solid solutions at low temperatures. *Journal of Thermal Analysis and Calorimetry*, 2019, **138(1):** 265–272.

微波烧结制备 ZrO_2-AlN 复合陶瓷的微观结构与性能研究

牟庭海[1,2]，许文涛[2,3]，凌军荣[2]，董天文[2]，秦梓轩[2]，周有福[2,3]

(1. 福建师范大学 化学与材料学院，福州 350007; 2. 中国科学院 福建物质结构研究所，光电材料化学与物理重点实验室，福州 350002; 3. 福建光电信息科技创新实验室，福州 350108)

摘 要：氧化锆(ZrO_2)陶瓷具有出色的机械性能，但其应用受到低热导率(Thermal Conductivity, TC)的限制。本研究设计并通过微波烧结制备了高热导率氧化锆–氮化铝(AlN)复合陶瓷，优化制备条件后，抑制了两种物质之间的反应，获得了致密的复合陶瓷(相对密度>99%)，详细研究了该复合陶瓷的组织演变、热学性能和力学性能。研究结果表明，随着 AlN 含量的增加，复合陶瓷的室温下热导率、热扩散系数和热容增加，分别达到 41.3 W/(m·K)、15.2 mm^2/s 和 0.6 J/(g·K)。这种具有高热导率和抗热震性的 ZrO_2-AlN 复合复合陶瓷在能源系统的高温热交换材料领域具有广阔的应用前景。

关 键 词：氧化锆；氮化铝；复合陶瓷；微波烧结；热导率

中图分类号：TQ174 **文献标志码：**A